

A Panoramic 3D Vision System from Multiple RGBD Sensors

Hang Liu¹, Hengyu Li^{1*}, Xiahua Liu², Jun Luo¹, Shaorong Xie¹, Yu Sun^{1,3}

Abstract—This letter presents a panoramic 3D vision system that was designed specifically for mapping the indoor environment. The system consists of multiple RGBD sensors that cover a 360° field of view, simplifying the reconstruction of indoor environments. A new extrinsic calibration approach is proposed to estimate the relative poses between the RGBD sensors. This approach relies on well-matched keypoints from a descriptor-based pattern, in this case, of a minimally overlapping field of view between sensors. A distributed capturing system was also designed to provide panoramic RGBD frames in real time. Experiments validate the accuracy of the proposed calibration approach and the efficiency of the proposed panoramic 3D vision system for indoor mapping.

I. INTRODUCTION

In recent years, indoor scene reconstruction and robot navigation have attracted much attention with the advent of low-cost and efficient depth and color (RGBD) devices such as the Microsoft Kinect, Intel RealSense, and Structure Sensor. The depth sensors of these devices can provide a depth map with a VGA resolution (640x480) at video-rate (e.g., 30 Hz) using efficient light-coding technology that avoids the challenging task of dense 3D reconstruction from color images. The 3D models reconstructed using these depth sensors have been used to generate more realistic 3D content for virtual reality (VR) and help align the rendered virtual objects with real scenes for augmented reality (AR). Furthermore, the direct depth sensing capability of these depth sensors are particularly suitable for helping robots manipulate and navigate in an unknown environment.

With an RGBD sensor, the simultaneous localization and mapping (SLAM)-based approach is mainly used for fusing the point cloud frames to reconstruct the indoor scenes [1], [2], [3]. However, hundreds or even thousands of frames must be captured in state-of-the-art SLAM systems to reconstruct a common indoor environment such as a room or an office [4] because of two problems:

1) The field of view (FOV) of depth sensors is limited; thus, only a small part of the scene is represented in a single

¹Hang Liu, Hengyu Li, Jun Luo, Shaorong Xie with the School of Mechatronic Engineering and Automation, Shanghai University, China. Hengyu Li is the corresponding author. scholar.hang@gmail.com lihengyu@shu.edu.cn

²Xiahua Liu with the Department of Engineering Mathematics, University of Bristol.

³Yu Sun with the Department of Mechanical and Industrial Engineering, University of Toronto, Canada, and the Shanghai University. sun@mie.utoronto.ca

This work was supported by the National Natural Science Foundation of China (grant numbers 61525305 and 61625304), the Shanghai Natural Science Foundation (grant numbers 17ZR1409700 and 18ZR1415300), and the basic research project of Shanghai Municipal Science and Technology Commission (grant number 16JC1400900).

frame. The Kinect, for example, has a horizontal FOV of 57°, which is much smaller than the horizontal 240° FOV of the Hokuyo URG-04LX-UG01, a laser scanner with a similar range and measurement accuracy compared with the Kinect [5].

2) To track the poses of depth sensors to effectively fuse multiple point cloud frames, consecutive captured frames should be captured to have sufficient scene overlap. Typically, more than ninety percent of overlap is required, which further increases the number of frames for reconstruction.

A solution to the problem is to use a multicamera setup in which the cameras face different directions to sample different sections of the environment. A typical multicamera setup consists of multiple color cameras [6], [7] or RGBD cameras [8], [9].

In this letter, we focus on a panoramic 3D vision system that consists of multiple RGBD sensors for indoor mapping. A new extrinsic calibration method that relies on a descriptor-based pattern to provide well-matched keypoints is proposed to estimate the relative poses between the RGBD cameras with minimal overlapping FoV. A distributed capturing system based on local area network (LAN) is also proposed to provide multiple RGBD frames in real time. The experiments using real scenes validate these features of our study.

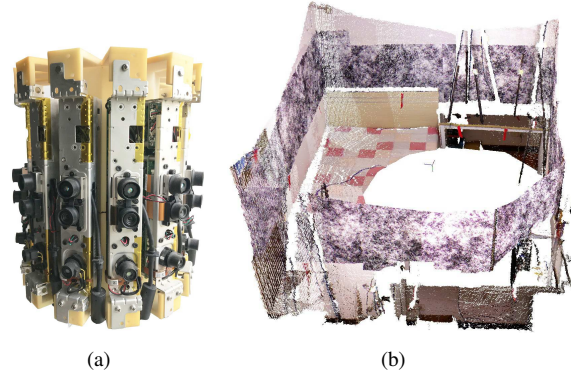


Fig. 1. (a) The setup used in this study for evaluating the proposed panoramic 3D vision system composed of 12 Kinect v1 RGBD sensors. (b) The panoramic 3D color point cloud obtained by the panoramic 3D vision system.

II. RELATED WORK

Panoramic cameras cover a wider field of view and therefore are applied in mapping systems to provide better localization constraints that can improve the accuracy of structure and motion estimation. One type of panoramic camera is the central catadioptric camera [10], which uses a combination of lenses and mirrors placed in a carefully

arranged configuration to capture a much wider FOV. This type of camera can capture 360° with a single camera and therefore is widely used in SLAM systems [11], [12]. Unfortunately, this type of camera has a poor and varying spatial resolution, lowering the measurement accuracy of a single camera pixel [13].

Another approach is to use a multicamera panoramic camera system. Although there are some complications from using multiple cameras, such as additional image data and more difficult calibration, the main advantage of a multicamera system is that it enables the construction of a high resolution 360° image. Studies using this type of multicamera systems appear in [14], [15].

SLAM systems that contain only color cameras can only compute sparse or semidense maps. However, applications such as augmented reality or obstacle avoidance for robots require a dense map of the environment. Thus, some range sensors are introduced in panoramic SLAM systems from laser range finders [11], [16] to stereo matching with triangulation [17] and structured light RGBD systems [18], [19]. Laser approaches are expensive and computing the depth from stereo image pairs is time-consuming. The structured light RGBD systems are low cost and have acceptable measuring accuracy in close ranges, which are suitable for direct 3D SLAM systems in indoor environments.

Complications can occur with the use of multiple cameras, such as more difficult calibration and additional image data. Fernandez-Moral et al. proposed to calibrate multiple RGBD sensors by finding and matching planes [8] or lines [20]. However, new algorithms for extracting and matching these planes or lines require redesign. The reason why classical extrinsic calibration strategies such as the chessboard-based method and the keypoints-based method cannot be applied is because the overlapping FoV between RGBD sensors cannot meet the overlap requirements of these methods. Chessboard-based methods require that chessboards be completely visible in the views of all cameras that must be calibrated. If the overlapping FoV is too small (e.g., thirty percent overlap), the overlapping image regions cannot provide correctly matched keypoints. Because the N number of cameras in a panoramic vision system provide N times the image data, it is also important to find effective ways to efficiently capture and transfer all the data.

In the following, we give the details of our calibration approach. Then, the multi-RGBD camera setup and a LAN-based distributed capturing system are presented in section IV. In addition, we analyze the precision of the proposed calibration approach and show the efficiency of indoor scene reconstruction using the proposed panoramic 3D vision system. Finally, the conclusions are summarized.

III. EXTRINSIC CALIBRATION

In this section, we address the problem of estimating extrinsic calibration (i.e., relative poses) between RGBD sensors that have little overlapping FoV. Fig. 1(a) shows a setup of the proposed panoramic 3D vision system that consists of 12 Kinect v1 sensors. All Kinects are vertically

positioned for a more compact design. The Kinect v1 sensor has an angular field of view (FoV) of 43° from the vertical. The overlap FoV of two neighboring sensors is only approximately 30 percent of the vertical FoV of each sensor.

We propose to solve the calibration problem of multiple RGBD sensor with little overlapping FoV using a feature descriptor-based calibration pattern [21], which can provide robust and accurate matched feature points in this case of minimal overlapping FoV. Based on these matched 2D feature points and depth maps from the depth sensors, we construct two 3D point sets to estimate poses by bundle adjustment. Then, a pose graph optimization method is used to refine the estimated poses.

A. Initial estimation of poses

The descriptor-based calibration pattern is composed of several noise images at different scales in accordance with the mechanism of SIFT/SURF. Compared with natural scenes, this pattern contains a high number of detectable features that can be easily detected by a camera at varying distances. Thus, the descriptor-based pattern can provide many and more accurately matched keypoints between two cameras in the case of minimal overlapping FoV.

In Fig. 2(a), the detected SURFT keypoints of such a pattern is represented by green circles. Fig. 2(c) shows the feature detection results of a nature scene. There are many more keypoints in Fig. 2(a). Fig. 2(b) and Fig. 2(d) show the matched keypoints of a pair of images captured by two cameras with an approximately thirty percent overlapping FoV. Well-matched keypoints are connected by green lines; poorly matched keypoints are connected by red lines. The matching results are generated by the Flann-based descriptor matcher implemented in OpenCV, where matched keypoints are accepted only if its descriptor distance is less than 2.0 times the minimum descriptor distances. Fig. 2(b) shows that the descriptor-based pattern provides more well-matched keypoints. In this work, the keypoints detector can only be applied to the overlapping regions of neighboring images to reduce the possibility of mismatch.

Then, based on these matched keypoints, we must find their corresponding depth values from the depth maps generated by the depth camera in the RGBD sensor to construct 3D point sets to estimate the poses. Due to the different spatial positions and intrinsic parameters of the IR camera of the depth sensor and of the color camera in the RGBD sensor, the depth map is not aligned with the color image. Because the depth and color cameras share enough overlapping FoV to detect the entire chessboard, we use the highly accurate chessboard calibration method to obtain the relative poses between the color and depth camera and their intrinsic parameters to align the depth map with the color image.

Let $[u, v]$ represent the coordinates of a keypoint, Z represents its depth value in $[u, v]$ of corresponding aligned depth map, and $[X, Y, Z]^T$ represent the 3D point of $[u, v]$ in the color camera coordinate system. According to the pinhole

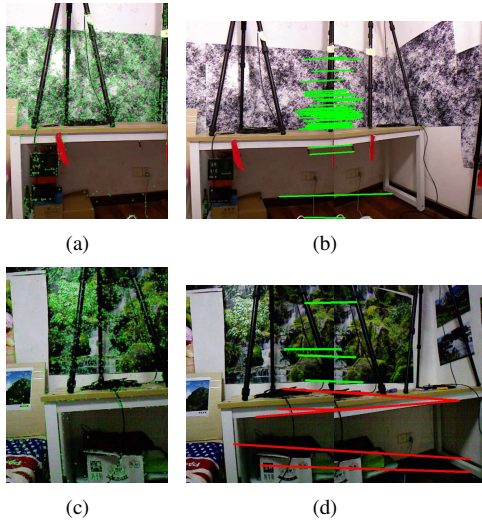


Fig. 2. (a) and (b) show the detected and matched keypoints of the image pairs with a descriptor-based pattern, respectively. (c) and (d) show the evaluation results of the image pairs with natural scenes. Keypoints are represented by green dots, well-matched keypoints are connected with green lines, poorly matched keypoints are connected with red lines.

camera model, the values of X and Y can be calculated as

$$\begin{aligned} X &= (u - u_0)Z/f_x, \\ Y &= (v - v_0)Z/f_y. \end{aligned} \quad (1)$$

We obtain two 3D point sets $\{p_i\}$, $\{p'_i\}$; $i = 1, 2, \dots, N$, based on (1). p_i and p'_i are 3×1 column matrices. The relative poses between these two 3D point sets can be found by minimizing

$$\min_{\xi} = \frac{1}{2} \sum_{i=1}^n \| (p'_i - \exp(\xi^{\wedge}) p_i) \|, \quad (2)$$

where $\xi \in se(3)$ is a vector with six dimensions that represents the camera pose, \wedge maps ξ to a matrix with four mentions $R^{4 \times 4}$. ξ^{\wedge} is mapped to $T \in SE(3)$ by the exponential map $\exp()$. We use bundle adjustment to jointly solve all camera poses [22]. The derivative with respect to the camera pose of an error element is given by

$$- (\exp(\xi^{\wedge}) p)^{\wedge} \quad (3)$$

where \wedge denotes the mapping from $\exp(\xi^{\wedge}) p$ represented by $[x, y, z]^T$ to corresponding antisymmetric matrix $\begin{bmatrix} 0 & -z & y \\ z & 0 & -x \\ -y & x & 0 \end{bmatrix}$, the detailed derivation process can be found in the appendices.

B. Pose Graph Optimization

Assume that there are N RGBD sensors in the panoramic 3D vision system. Let $T_{i,j}$ denote the estimated relative poses between two adjacent RGBD sensors, $i = 1, 2, \dots, N$; $j = i + 1$, when i equals N , j is 1. When the pose of the first RGBD sensor is set to $[0, 0, 0, 1]^T$, we can calculate the pose x_i for each RGBD sensor based on $T_{i,j}$. Due to the pose estimation error, the pose that is calculated by $T_{N,1}x_N$ is not equal to $[0, 0, 0, 1]^T$. Fortunately, this panoramic setup of

RGBD sensors provides a definite loop-closure constraint for optimizing the estimated poses. We can solve this problem by using the popular pose graph optimization method in SLAM [22].

According to pose graph optimization theory, the problem can be solved by finding the minimum of a function of this form:

$$x^* = \arg \min_x \sum_{(i,j) \in S} r_{i,j}^T(x) \Lambda_{i,j} r_{i,j}(x), \quad (4)$$

where $x = (x_1^T, \dots, x_n^T)^T$ is a vector of poses, $r_{i,j}$ is the residual of the predicted and observed relative poses between the i -th and j -th node, $\Lambda_{i,j}$ denotes the measurement information matrix, and S represents the set of edges that connect the nodes.

IV. EXPERIMENTS AND RESULTS

In this section, we evaluate the accuracy of the proposed extrinsic calibration method and show the efficiency of constructing indoor environments using the panoramic 3D vision system.

A. System Setup

We designed a camera rig that consists of twelve Kinect v1 RGBD sensors mounted in a radial configuration (see Fig. 1(a)). We also designed a distributed system built on top of a local area network (LAN) to capture the RGBD frames from all twelve sensors in real time. The distributed capturing system (see Fig. 3) comprises twelve Raspberry Pi single board computers, a gigabit switch and a high-performance computer. Raspberry Pi is used to obtain the RGBD frames from each Kinect and send the data to the high-performance computer through the LAN using User Datagram Protocol. The high-performance computer is used to receive and process the RGBD frames. Both the depth and color frames are set to a size of 640×480 ; the values of a single pixel in the depth frame and color frame have a size of 2 bytes and 3 bytes, respectively. Thus, the size of the RGBD frames from all twelve Kinects is 17.58 million bytes, which can be sent to the high-performance computer through the gigabit switch at 7 fps. This frame rate can be increased by decreasing the size of RGBD frames from Kinect.



Fig. 3. Distributed capturing system consisting of a gigabit switch and 12 low-cost Raspberry Pi single board computers.

B. Precision of Extrinsic Calibration

To evaluate the precision of the proposed extrinsic calibration method, we use a motion capture system to obtain the ground truth relative poses between the sensors. The motion capture system requires at least three reflective markers to track the pose of a rigid body, such as the Kinect and the chessboard in our experiments. We attached four reflective markers to both the Kinect and the chessboard (see Fig. 4). We placed the four markers on the outer corners of the chessboard, such that the relative poses between the chessboard and the motion capture system and the Kinect color camera are known. The motion capture system can track the poses of the markers that are attached to the Kinect to determine the poses of the Kinect color camera.

For convenience, we only attached markers to one Kinect and placed this Kinect on twelve different positions in the camera rig to capture RGBD frames. The precision of the extrinsic calibration is evaluated using twelve pairs of RGBD frames from the captured twelve RGBD frames.

While determining the keypoints correspondences for each pair of RGBD frames, we increase the distance threshold of the keypoints (denoted by $dist_thresh$) from one and a half times the minimum distance to the maximum distance (ten times the minimum distance in average) to analyze the calibration error in rotation and translation with respect to the keypoints correspondences.

In TABLE I, the average residual error in rotation and translation is presented for the initial estimation (denoted by Ini.) and optimized estimation (denoted by Opti.) using pose graph optimization with loop closure. It can be seen that the average residual error is reduced when raising the distance threshold to consider more keypoint correspondences. The residual error in both the rotation and translation for the optimized estimation is generally less than the residual error for the initial estimation. When the distance threshold is set to be larger than four times the minimum distance, the residual error remains at the same level. The aligned point clouds before and after pose graph optimization with loop closure can also be observed in Fig. 5. It can be seen in the red circle on the bottom of Fig. 5(a) that the point clouds are misaligned, however, these point clouds align well in Fig. 5(b) with optimized poses with loop closure constraint.

The operating range of the Kinect v1 depth sensor is between 0.5 m to 5.0 m [23]. Using an output panoramic frame can reconstruct scenes within the circle with a radius of 5 meters. Thus the reconstruction of some indoor scenes becomes very efficient using the proposed panoramic 3D vision system. Fig. 6 presents the reconstruction result of a bedroom (3.3 m \times 3 m) and a living room (9 m \times 3.5 m) using only one output panoramic frame from the proposed system.

V. CONCLUSION

In this letter, we present a panoramic 3D vision system from multiple RGBD sensors. A new methodology that relies on well-matched keypoints provided by a feature descriptor-based calibration pattern has been proposed to

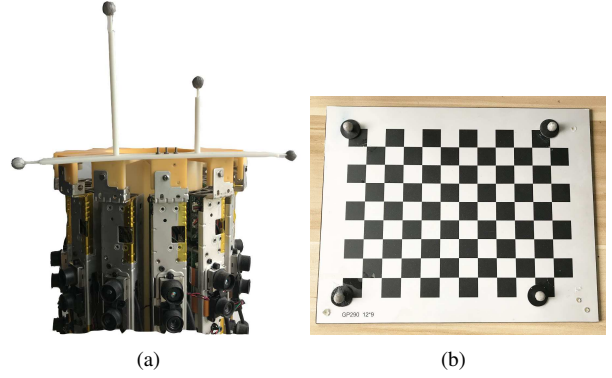


Fig. 4. (a) Kinect with reflective markers. (b) Chessboard with reflective markers.

calibrate the extrinsic parameters of the RGBD sensors in the system. We have also designed a LAN-based distributed system that enables the system to provide panoramic RGBD frames in real time. The reconstruction of indoor scenes is efficiently and conveniently performed using this panoramic 3D vision system considering the time consumption and captured RGBD frames. All the experiments have validated the accuracy of the proposed calibration method and the efficiency in reconstruction.

Directions for future work include research on integrating the proposed panoramic 3D vision system with state-of-the-art SLAM systems for localization and mapping at large scales. The proposed system provides a 360° FoV, leading to better constraints for localization and can be potentially used to reduce localization and mapping errors. It is particularly important to investigate direct registration methods such as [24], [25], which do not depend on time-consuming keypoint detectors or descriptors for large scale SLAM, using this panoramic 3D vision system.

APPENDIX

The detailed derivation process of the derivative with respect to the camera pose of a error element is as follows,

$$\begin{aligned}
 \frac{\partial(\exp(\xi^*)p)}{\partial\xi} &= \lim_{\delta\xi\rightarrow 0} \frac{\exp(\delta\xi^*)\exp(\xi^*)p - \exp(\xi^*)p}{\delta\xi} \\
 &\approx \lim_{\delta\xi\rightarrow 0} \frac{(I + \delta\xi^*)\exp(\xi^*)p - \exp(\xi^*)p}{\delta\xi} \\
 &= \lim_{\delta\xi\rightarrow 0} \frac{\delta\xi^*\exp(\xi^*)p}{\delta\xi} = \lim_{\delta\xi\rightarrow 0} \frac{-(\exp(\xi^*)p)^*\delta\xi}{\delta\xi} \\
 &= -(\exp(\xi^*)p)^*
 \end{aligned} \tag{5}$$

TABLE I
RESIDUAL ERRORS OF INITIALLY ESTIMATED POSES AND OPTIMIZED POSES

<i>dist_thresh/min_dist</i>	1.5	2	3	4	5	6	7	8	9	10
Correspondences	14	56	218	373	477	568	615	631	642	651
Ini. rot error(deg)	2.07	1.48	1.40	1.48	1.51	1.53	1.51	1.52	1.52	1.52
Opti. rot error(deg)	1.96	0.89	0.76	0.62	0.61	0.56	0.56	0.56	0.56	0.56
Ini. trans error(cm)	9.25	2.73	1.86	2.07	2.07	1.81	1.80	1.81	1.80	1.81
Opti. trans error(cm)	4.94	2.78	1.88	1.84	1.77	1.83	1.83	1.81	1.82	1.80

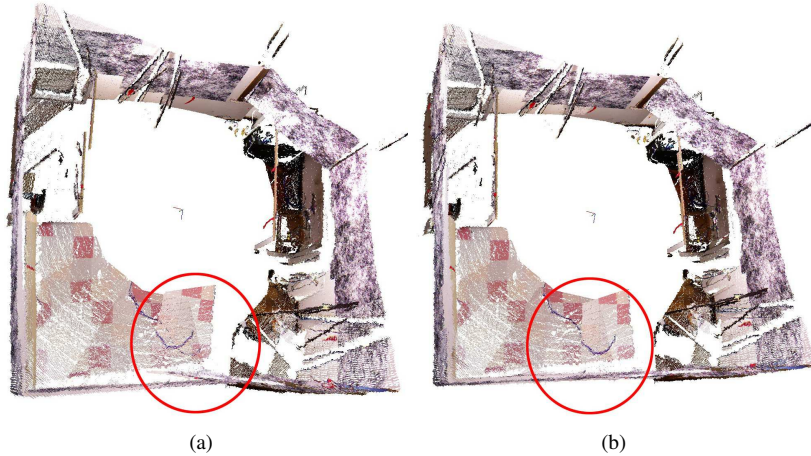


Fig. 5. The aligned point clouds before (a) and after (b) closing the loop. A miss alignment can be observed in the red circle on the bottom of (a). After the pose graph optimization with loop closure, this miss alignment is resolved.

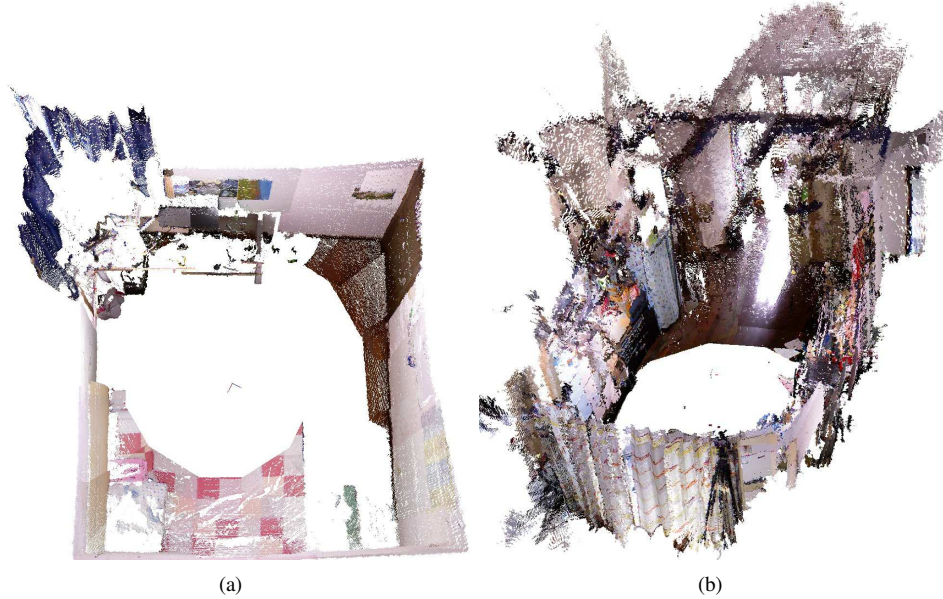


Fig. 6. Reconstruction of a bedroom (3.3 m \times 3 m) (a), and a living room (9 m \times 3.5 m) using only one output frame from the proposed panoramic 3D vision system.

REFERENCES

- [1] R. Mur-Artal and J. D. Tardos, "Orb-slam2: An open-source slam system for monocular, stereo, and rgbd cameras," *IEEE Transactions on Robotics*, vol. 33, no. 5, pp. 1255–1262, 2017.
- [2] T. Whelan, R. F. Salas-Moreno, B. Glocker, A. J. Davison, and S. Leutenegger, "Elasticfusion: real-time dense slam and light source estimation," *The International Journal of Robotics Research*, vol. 35, no. 14, pp. 1697–1716, 2016.
- [3] C. Kerl, J. Sturm, and D. Cremers, "Dense visual slam for rgbd cameras," in *2013 IEEE/RSJ International Conference on Intelligent Robots and Systems*, 2013, pp. 2100–2106.
- [4] J. Sturm, N. Engelhard, F. Endres, W. Burgard, and D. Cremers, "A benchmark for the evaluation of rgbd slam systems," in *Proc. of the International Conference on Intelligent Robot Systems (IROS)*, Oct. 2012.
- [5] S. Zug, F. Penzlin, A. Dietrich, T. T. Nguyen, and S. Albert, "Are laser scanners replaceable by kinect sensors in robotic applications?" in *Robotic and Sensors Environments (ROSE), 2012 IEEE International Symposium on*. IEEE, 2012, pp. 144–149.
- [6] L. Heng, G. H. Lee, and M. Pollefeys, "Self-calibration and visual slam with a multi-camera system on a micro aerial vehicle," *Autonomous Robots*, vol. 39, no. 3, pp. 1–19, 2015.
- [7] M. J. Tribou, A. Harmat, D. W. L. Wang, I. Sharf, and S. L. Waslander, "Multi-camera parallel tracking and mapping with non-overlapping fields of view," *International Journal of Robotics Research*, vol. 34, no. 12, 2015.
- [8] E. Fernandez-Moral, J. Gonzalez-Jimenez, P. Rives, and V. Arevalo, "Extrinsic calibration of a set of range cameras in 5 seconds without pattern," in *Ieee/rsj International Conference on Intelligent Robots and Systems*, 2014, pp. 429–435.
- [9] P. Rives, "Scene structure registration for localization and mapping," *Robotics and Autonomous Systems*, vol. 75, no. PB, pp. 649–660, 2016.
- [10] S. K. Nayar, "Catadioptric omnidirectional camera," in *Proceedings of IEEE Computer Society Conference on Computer Vision and Pattern Recognition*, 1997, pp. 482–488.
- [11] C. Zou, B. He, L. Zhang, J. Zhang, and Z. Deng, "An automatic calibration between an omni-directional camera and a laser rangefinder for dynamic scenes reconstruction," in *2016 IEEE International Conference on Robotics and Biomimetics (ROBIO)*, 2016, pp. 1528–1534.
- [12] M. Schnbein and A. Geiger, "Omnidirectional 3d reconstruction in augmented manhattan worlds," in *2014 IEEE/RSJ International Conference on Intelligent Robots and Systems (IROS 2014)*, 2014, pp. 716–723.
- [13] Z. Zhang, H. Rebucq, C. Forster, and D. Scaramuzza, "Benefit of large field-of-view cameras for visual odometry," in *2016 IEEE International Conference on Robotics and Automation (ICRA)*, 2016, pp. 801–808.
- [14] M. Kaess and F. Dellaert, "Probabilistic structure matching for visual slam with a multi-camera rig," *Computer Vision and Image Understanding*, vol. 114, no. 2, pp. 286–296, 2010.
- [15] J.-P. Tardif, Y. Pavlidis, and K. Daniilidis, "Monocular visual odometry in urban environments using an omnidirectional camera," in *2008 IEEE/RSJ International Conference on Intelligent Robots and Systems*, 2008, pp. 2531–2538.
- [16] P. D. Gashgore, K. Kawasue, K. Yoshida, and R. Aoki, "Indoor space 3d visual reconstruction using mobile cart with laser scanner and cameras," in *Eighth International Conference on Graphic and Image Processing (ICGIP 2016)*, vol. 10225, 2017.
- [17] M. Meilland, A. I. Comport, and P. Rives, "Dense omnidirectional rgbd mapping of large-scale outdoor environments for real-time localization and autonomous navigation," *Journal of Field Robotics*, vol. 32, no. 4, pp. 474–503, 2015.
- [18] T. Gokhool, R. Martins, P. Rives, and N. Despre, "A compact spherical rgbd keyframe-based representation," in *2015 IEEE International Conference on Robotics and Automation (ICRA)*, 2015, pp. 4273–4278.
- [19] T. Gokhool, M. Meilland, P. Rives, and E. Fernandez-Moral, "A dense map building approach from spherical rgbd images," in *2014 International Conference on Computer Vision Theory and Applications (VISAPP)*, 2014, pp. 656–663.
- [20] A. Perez-Yus, E. Fernandez-Moral, G. Lopez-Nicolas, J. J. Guerrero, and P. Rives, "Extrinsic calibration of multiple rgbd cameras from line observations," *IEEE Robotics and Automation Letters*, vol. PP, no. 99, pp. 1–1, 2017.
- [21] B. Li, L. Heng, K. Koser, and M. Pollefeys, "A multiple-camera system calibration toolbox using a feature descriptor-based calibration pattern," in *Ieee/rsj International Conference on Intelligent Robots and Systems*, 2014, pp. 1301–1307.
- [22] R. Kummerle, G. Grisetti, H. Strasdat, K. Konolige, and W. Burgard, "G 2 o: A general framework for graph optimization," pp. 3607–3613, 2011.
- [23] K. Khoshelham and S. O. Elberink, "Accuracy and resolution of kinect depth data for indoor mapping applications," *Sensors*, vol. 12, no. 2, p. 1437, 2012.
- [24] J. Engel, V. Koltun, and D. Cremers, "Direct sparse odometry," *IEEE transactions on pattern analysis and machine intelligence*, vol. 4, 2017.
- [25] C. Forster, M. Pizzoli, and D. Scaramuzza, "Svo: Fast semi-direct monocular visual odometry," in *Robotics and Automation (ICRA), 2014 IEEE International Conference on*. IEEE, 2014, pp. 15–22.